POAC'23
Glasgow, United Kingdom

Proceedings of the 27th International Conference on
Port and Ocean Engineering under Arctic Conditions
12-16 June 2023, Glasgow, United Kingdom

Modelling of ice-interaction with a sea channel marker in the Bothnian Bay

Jaakko Heinonen[1], Eeva Mikkola[1]
[1] VTT Technical Research Centre of Finland Ltd., Espoo, Finland

ABSTRACT

The Gulf of Bothnia freezes every winter. At times, the level ice thickness in the northern part reaches close to 1 m. In that sea area the ice usually introduces the most significant uncertainty for the design of offshore structures. Drifting level ice induces a dynamic load on the structure, which needs to be designed carefully to avoid harmful vibrations. Implementing an inclined element at the structure water line is a promising solution to mitigate ice loads and ice-induced vibrations. This presentation introduces the modelling of ice-interaction with a bottom-fixed sea channel marker, a slender monopile structure located by the 12.5 m deep waterway to Oulu, in the Bothnian Bay. The height of the structure is 12 m above the water line. The structure is implemented with a cone having a waterline diameter of 3 m at the mean water level. A structural model for the sea channel marker was created including the soil-structure interaction model. Dynamic ice loads were created by combining analytical models to determine the load peaks and previous full-scale and model-scale tests to determine the frequency of the load peaks. Case studies were carried out to study how the structural acceleration responses depend on the ice thickness and ice velocity. The kinematic responses were analysed to find out a correlation between the accelerations at the selected locations in the structure and the ice load. This information is crucial for finding optimal locations for acceleration sensors when planning the test set-up for full-scale measurements.

KEY WORDS: Ice loads, channel marker, ice-induced vibration, cone

INTRODUCTION

Full-scale measurements of sea ice loads on offshore structures are crucial for increased understanding of the ice-structure interaction process and how the ice load develops. Measurements are also important for validating the ice load models used for the design of structures.

In the past, some lighthouses and winter channel markers in the Bothnian bay have been implemented by ice load measurements. In the lighthouse Norströmsgrund, the ice load was measured directly at the ice contact on the cylindrical structure by using ice load panels. Full-scale measurements were carried out from 1998 to 2004. These measurements have been studied thoroughly in numerous studies, e.g. Bjerkaas (2006), Bjerkaas and Nord (2016), Li et al. (2016) and Nord et al. (2018).

The measurements in Kemi-1 lighthouse were carried out in winters 1984/85 and 1985/86, which were some of the harshest winters in the past century. A conical mantel was built on top of the original cylindrical caisson type foundation, where the ice loads were measured by pneumatic devices. Analyses of these measurements have been published by Hoikkanen (1985), Määttänen (1986), Määttänen and Mustamäki (1985) and Brown and Määttänen (2009).

Björnklack offers an important learning about the risks due to sea ice loads (Bjerkaas and Nord, 2016). In 1986 the lighthouse Björnklack - in the Swedish side of the Bothnian Bay -suffered very high ice loads and the gravity-based foundation was not able to withstand the loads. The whole lighthouse slid along the seabed and the structure tilted heavily. Later, the lighthouse was demolished and replaced by a buoy.

Nordlund et al. (1988) and Turunen & Nordlund (1988) carried out measurements of ice-induced vibrations on the channel marker offshore Kokkola in the Bothnian Bay. Even though the monopile itself was slightly conical, the ice was mostly failing by crushing. The structure was not implemented by an ice breaking cone.

Nord at al. (2015) presented plans for Hanko-1 channel marker to monitor the ice forces in the Gulf of Finland. They suggested a sensor network consisting of accelerometers and strain gages to identify ice forces. However, due to warm and ice-less winters, the measurements have not taken place so far. Figure *1* indicates the locations of the lighthouses and channel markers mentioned above.

In the current study we aim to implement one of the winter channel markers – Kiisla – with an ice load measurement system that would also include profiling of the ice thickness and velocity. Kiisla is located in the Bothnian Bay, North-West from Hailuoto island. In that area ice is drifting most of the winter season. The measurements are planned for incoming two winters. We aim to measure the ice geometry interacting with structure and synchronize it with the structural response. For planning the test set-up for these full-scale measurements, we studied the structural performance of the channel marker. The target is to place acceleration sensors at optimal locations in the structure. To be able to simulate the dynamic response of the structure, we need to model the structure with soil-structure-interaction. As the ice load is acting at the water level and the accelerometers must locate in a dry place above the water level, we'll need to determine the correlation between the excitation force and kinematic response at selected locations.

In the long term, we aim to promote a full-scale offshore wind turbine demonstration foundation in real operational environment, see the position paper by Hoyland et al. (2023). The target is to validate theoretical and numerical models for the structural design purposes and to develop reliable and cost-efficient foundations precisely for wind turbines in ice conditions.

Figure 1. Locations of structures that have been used for ice load measurements. Lighthouses are shown by dark green dots and channel markers with red dots. Kiisla is the channel marker for the present study. Map data from OpenStreetMap.

NUMERICAL MODEL

Structural model

The foundation of the channel marker is a steel monopile, that was piled into the seabed and implemented by an ice breaking cone at the water line to mitigate ice loads. The monopile was filled by sand and the cone was filled by concrete. The cone angle is 60 degrees and the water depth at the site is 15 m as shown in Figure *2*. Main dimensions of the model are shown in Table *1*. Material properties used to model the structure and added mass damping are shown in Table 2.

Table 1. Main dimensions of the channel marker.

Parameter description	Value
Cone angle	60 deg
Height from the mean water level	12 m
Top level of the ice breaking cone	1.5 m
Lower level of the upward breaking cone	-1.5 m
Lower level of the downward breaking cone	-2.0 m
Sea bottom	-14.9 m
Depth of monopile from the MWL	-35.0 m
Waterline diameter (m)	3.0
Monopile diameter (in seabed)	4.19 m
Diameter of the tower (above the cone)	0.83 m

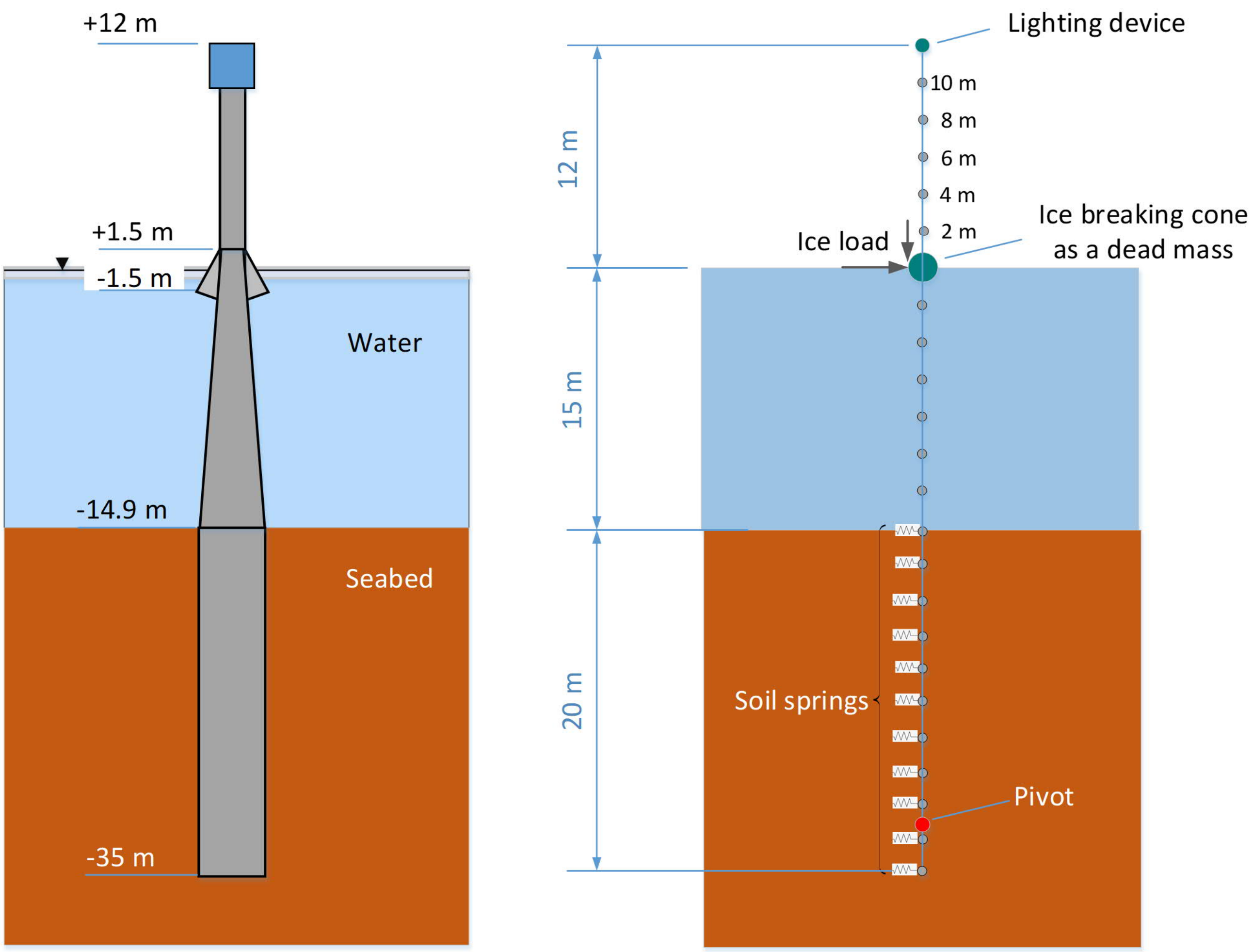

Figure 2. Left: A schematic illustration of the channel marker structure with main dimensions. Right: Beam-lumped mass model with the soil interaction and ice load.

Table 2. Material properties used in the structural model.

Material	Parameter	Symbol	Value	Unit
Steel	Elastic modulus	E	200	GPa
	Shear modulus	G	79.3	GPa
	Density	ρ	7850	kg/m3
Water	Density	ρ	1000	kg/m3
Soil	Density	ρ	2200	kg/m3
Concrete	Density	ρ	2400	kg/m3

Commercial finite element software Simulia/Abaqus 2022 was applied for the dynamic simulations. Three-dimensional structural model of the channel marker and its foundation consisted of beam elements. Mass elements were applied to model added mass damping for submerged region and spring elements for the soil-structure interaction. Total number of variables in the model was 1416.

Damping

Various sources of damping: structural, soil, and hydrodynamic were estimated. Structural damping in time-domain dynamic analyses was modelled by Rayleigh damping factors: α for mass proportional damping and β for stiffness proportional damping. α and β were determined so that they correspond to damping ratios of 1% at two lowest natural frequencies. Damping ratio was given in percentage of critical damping.

Damping in the structural parts below the water level was modelled by an added mass method. Amount of mobilized volume is assumed equal to half of the submerged monopile volume. The same assumption was used for the part dug into seabed. Added mass elements were distributed vertically with 1 m intervals.

Soil-structure interaction

Seabed properties are based on the information from the foundation designer. The seabed consists of layers of frictional soil. Therefore, the material properties vary and depend on the depth. The soil-structure interaction was modelled by springs connected with the monopile and distributed vertically with 1 m intervals. A simplified model commonly used for bridge design was used to determine individual spring stiffnesses.

DYNAMIC ICE LOAD EXCITATION

Dynamic ice load model is based on the bending failure of an ice field on a cone. The interaction between the moving ice field and the cone causes time varying cyclic horizontal and vertical forces. The time variation depends on the velocity and the critical breaking length of the moving ice field. The interaction between the cone and the moving ice field was divided into three phases: loading, unloading and gap phases. At the loading phase the cone interacts with the moving ice field causing an increase in the horizontal and vertical force. Due to bending failure of the ice field, the horizontal and the vertical forces decrease in unloading phase from the peak value to residual levels as visualized in Figure 3. The maxima of the ice load components were calculated according to the standard ISO 19906 (2019), where the horizontal action component is determined as

$$F_H = \begin{cases} (H_{B1} + H_R + H_P + H_L + H_T) I_{p1} \\ (H_{B1} + H_R + H_P + H_L + H_T) I_{p2} \end{cases} \quad (1)$$

Where H_{B1} and H_{B2} are the horizontal force components corresponding to the first and the second breaking of the ice, H_R is the horizontal force component to push the broken ice blocks upwards along the cone, H_P is the force component required to push the sheet ice through the accumulated ice pile, H_L is the horizontal force component required to lift the ice rubble on top of the advancing ice sheet prior to breaking it, H_T is the horizontal force component to turn the ice block at the top of the cone when the ice contacts with the vertical face, and I_{p1} and I_{p2} are the correction factors for the effect of in-plane compression in the ice sheet due to horizontal force. The comprehensive set of equations for all of the components as well as the calculation method of the dynamic load signal can be found from ISO 19906 (2019).

The dynamic ice load excitation depends strongly on the ice thickness and velocity. Therefore, a parameter study was carried out with reasonable combinations of the ice thickness ranging from 0.1 to 0.8 m and velocity ranging from 0.1 to 0.2 m/s. Selected parameters do not necessarily represent the worst cases at the site, but are definitely harsh enough to demonstrate ice-induced vibrations. Ice parameters used for the calculations are shown in Table 3. The maximum loads for different ice thicknesses are collected in Table 4.

Table 3. Input parameters for drifting level ice.

Quantity	**Value**
Thickness of the ice	[0.1, 0.2, 0.3, 0.4, 0.5, 0.6, 0.7, 0.8] m
Ice velocity	[0.1, 0.2] m/s
Ice ride-up height	2.70 m
Flexural strength of the ice sheet	0.60 MPa
Density of ice	930 kg/m3
Density of water	1011 kg/m3
Gravity acceleration	9.81 m/s2
Elastic modulus of ice	3.0 GPa
Poisson ratio for ice	0.33
Friction between ice and structure	0.10
Ice-ice friction (kinetic)	0.15
Angle of repose of broken ice	50°
Cohesion of ice rubble	7.0 kPa
Friction angle of ice rubble	35°
Porosity of ice rubble	0.30

Table 4. Maxima of horizontal ice loads for the drifting level ice for the cone angle of 60 degrees.

Ice thickness (m)	Horizontal ice load (kN)	Vertical ice load (kN)
0.1	119	51
0.2	172	74
0.3	245	105
0.4	359	154
0.5	501	214
0.6	672	287
0.7	872	373
0.8	1100	471

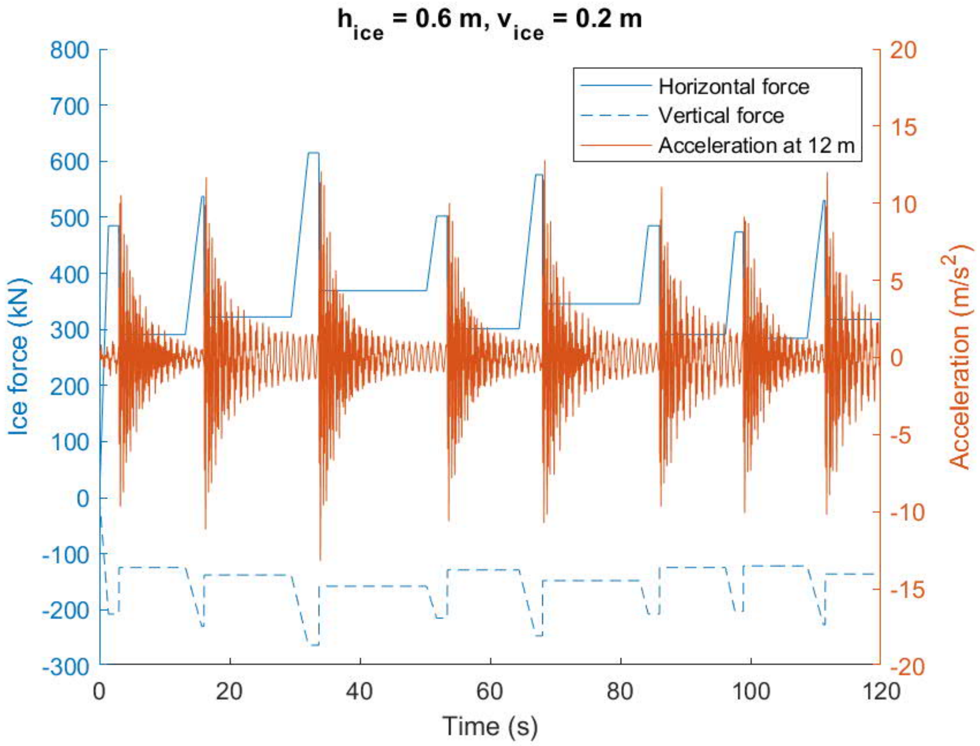

Figure 3. Time history plot of dynamic ice loads and acceleration response for ice velocity 0.2 m/s and ice thickness 0.6 m.

NUMERICAL SIMULATIONS

Natural frequencies

As the structure is symmetric in relation to x and z-axis, the lowest translational modes appear pairwise. Three lowest mode shapes with corresponding natural frequencies (1.06, 4.49 and 6.55 Hz) are shown in Figure *4*. The picture also shows vertical levels of 0, 4, 8 and 12 m in which the structural responses were analysed. In comparison, Turunen & Nordlund (1988) measured in Kokkola a channel marker with natural frequencies around 3.25 Hz and 6.43 Hz. Higher frequencies indicate that the foundation in Kokkola is stiffer compared to Kiisla, because of shallower water and different seabed properties.

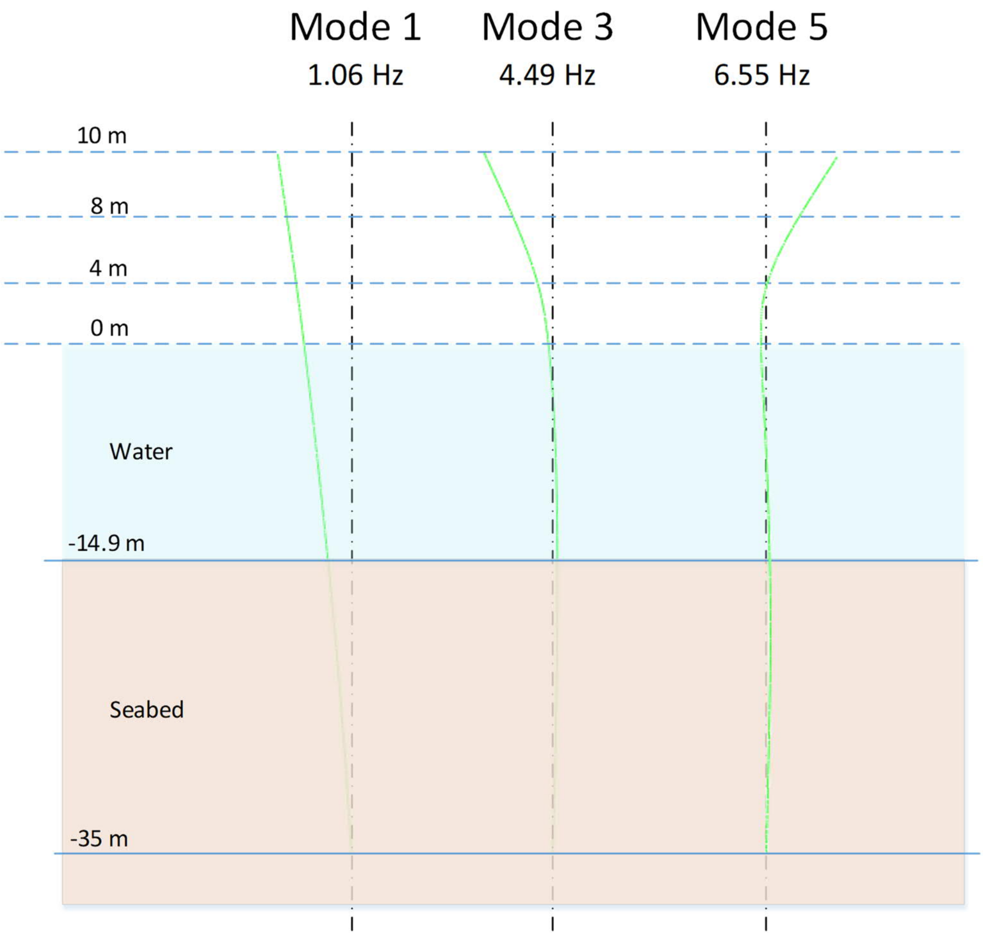

Figure 4. Natural mode shapes and frequencies of the channel marker. Three lowest modes in a vertical cross-section plane.

RESULTS

Kinematic response

Dynamic response (horizontal acceleration) in the channel marker was studied at selected vertical positions from the water line to the top of the structure. Figure 3 shows a typical time history of acceleration response with transient behaviour and highest peak-to-peak values right after the ice force drops. In the following analysis, impact refers to the unloading phase where the ice load drops from the peak value to a residual level, and response is given as peak-to-peak acceleration for each impact. The simulations were run with 0.001 s time step i.e. frequency of 1 000 Hz. The duration of the simulations was 120 s for all simulations with ice velocity of 0.2 m/s. For the lower ice velocity of 0.1 m/s the simulation duration was 200 s, except for the highest ice thickness of 0.8 m, where the simulation duration was 300 s. At least 5 impacts were obtained for all simulations.

Figure 5 shows the relationship between the ice impact and the channel marker vibration as a ratio of response divided by impact (in MN) and normalized with height. Figure 5a) and b) show that the ratio is independent of ice velocity and ice thickness. Ice velocity does however affect the number of impacts in a specific time frame: with decreasing ice velocity the number of impacts also decreases. The response-impact -ratio is mainly affected by the location: at 12 m, the ratio is between 2 and 2.5, whereas at 4 m, the ratio is between 1.75 and 3.5. The average ratio is similar at both vertical positions, but much higher variance is observed at 4 m height compared to 12 m height.

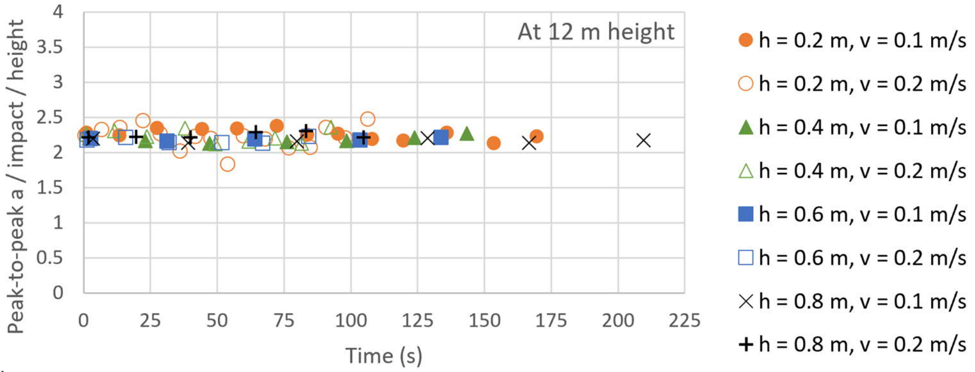

a)

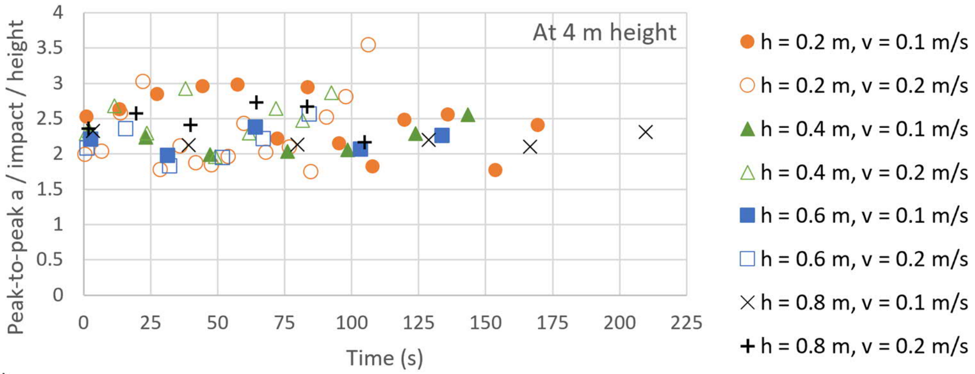

b)

Figure 5. Response-impact -ratio at two different vertical positions from water line. Normalized with respect to height.

Figure 6 shows the correlation between impact and response at four different vertical positions. All positions show good correlation between impact and response. Highest correlation is observed at 12 m height: R^2 is 0.9964. From 12 m, the correlation factor slowly decreases towards the water line level. This is shown also in Figure 7, where correlation is given as a function of height in 2 m intervals. At the same time, the maximum peak-to-peak acceleration decreases from 43 m/s^2 to 11 m/s^2 (see also Figure 6). These peak-to-peak accelerations are for 0.8 m ice thickness and 0.2 m/s ice velocity. Correlation weakens while acceleration level reduces.

To further explain the reduction in correlation, Figure 8 shows the frequencies observed at different vertical positions for one simulation with 0.6 m ice thickness and 0.2 m/s ice velocity. At 12 m, the 1st, 3rd and 5th mode are clearly present, with the highest power spectral density corresponding to the 3rd mode. At 8 m, the 5th mode is already starting to disappear and at 4 m and 0 m (water line), only the 1st mode is clearly present. This result is in line with the natural mode shapes shown in Figure *4*.

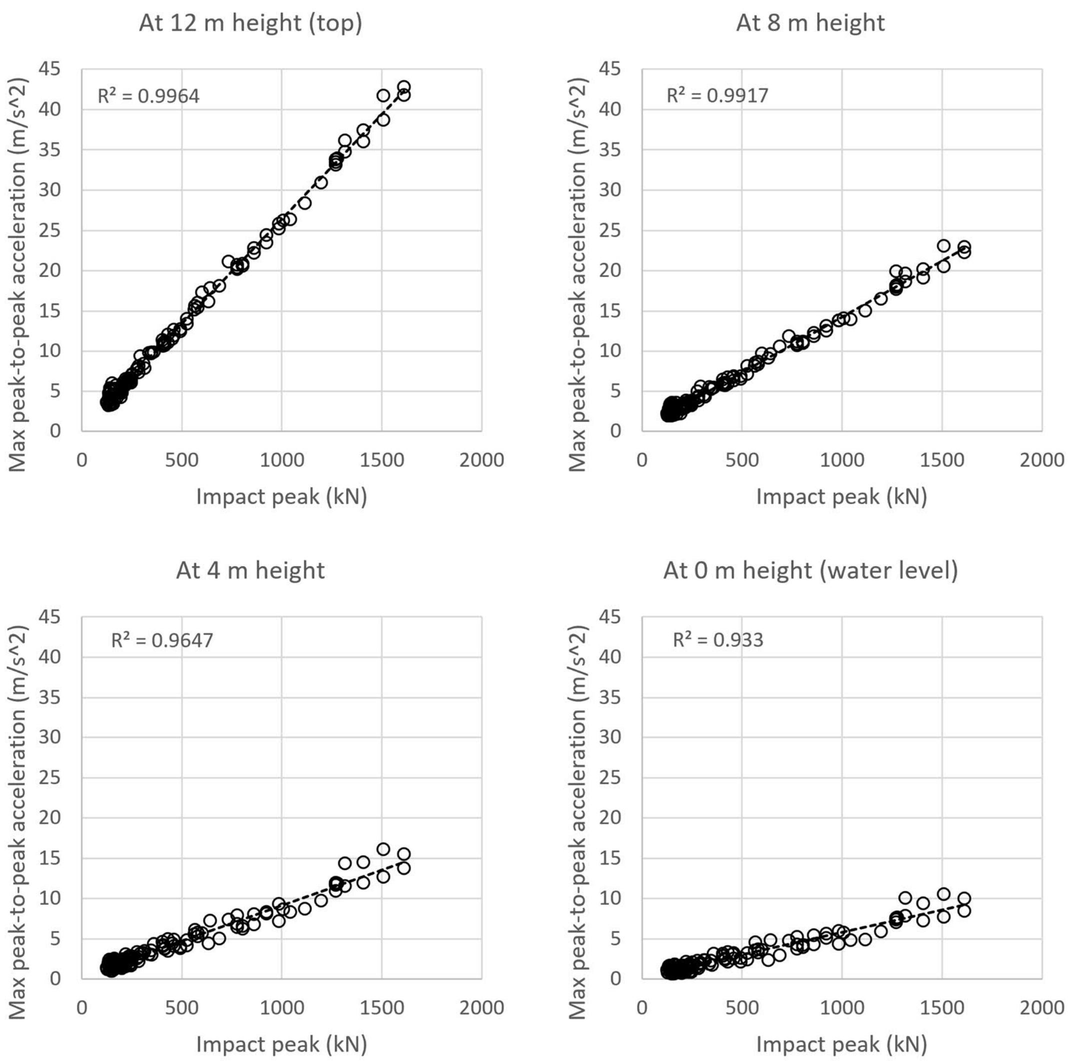

Figure 6. Impact-response correlation at different vertical positions from waterline.

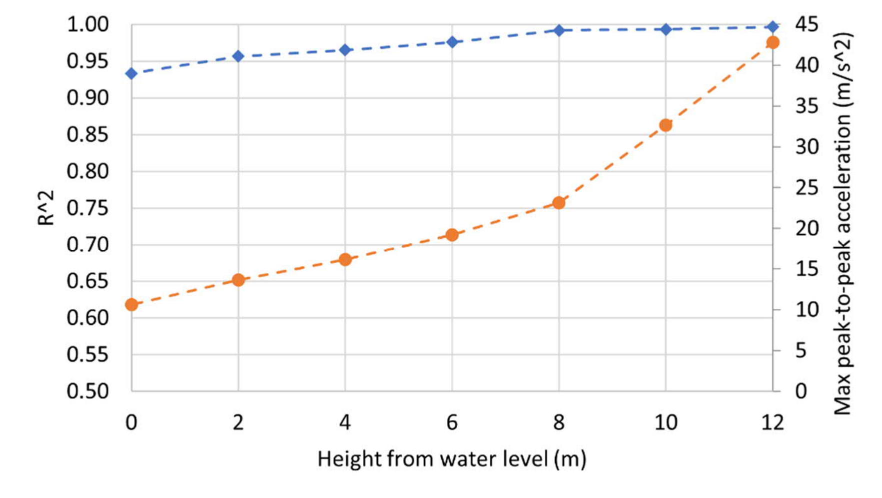

Figure 7. Impact-response correlation and maximum peak-to-peak values at different vertical positions from water level. The peak-to-peak accelerations are for 0.8 m ice thickness and 0.2 m/s ice velocity.

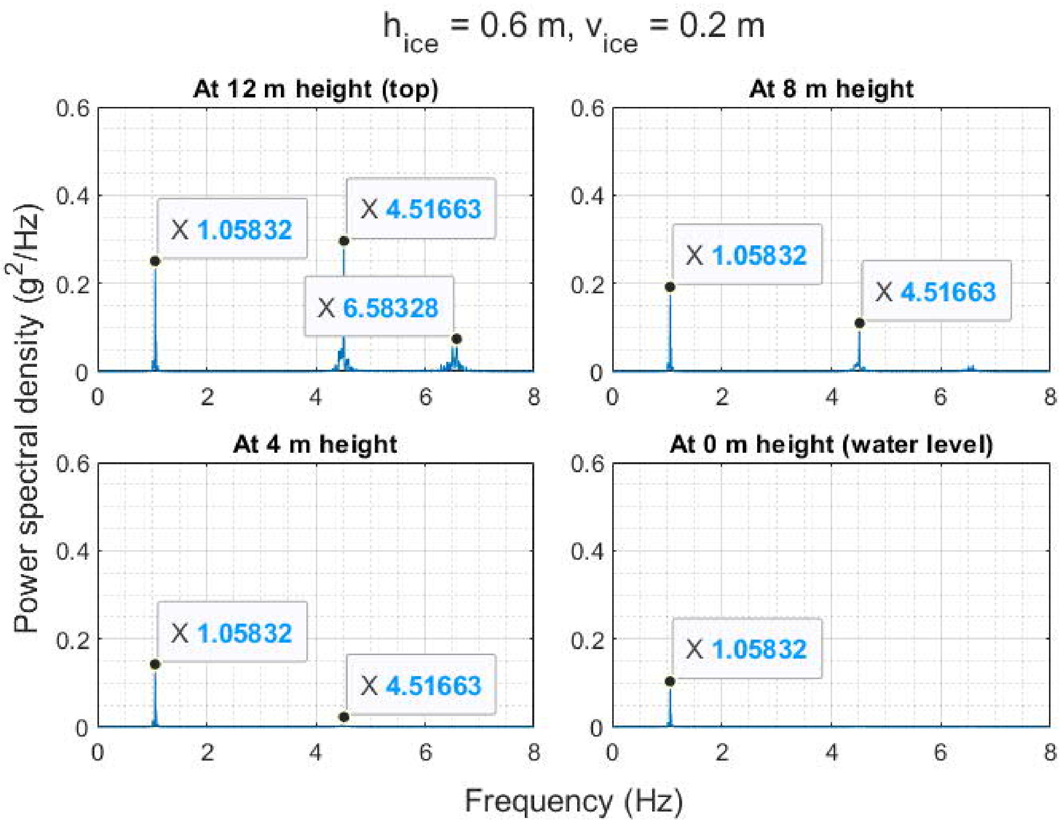

Figure 8. Frequencies observed in acceleration response at different vertical positions from water level.

CONCLUSIONS

A channel marker in the Northern Bothnian Bay was studied prior to full-scale ice load measurements in forthcoming winters. We aim to measure kinematic response above the water level of the structure in ice-interaction. For that purpose, we simulated dynamic ice load excitation on the structure and analysed horizontal acceleration response at the selected vertical positions in the structure. This information is important when finding optimal locations for acceleration sensors for full-scale measurements.

Best correlation between dynamic ice loads and acceleration response was found at 12 m, at the channel marker top. The peak-to-peak acceleration response was mainly dependent on the ice thickness, whereas the frequency of impacts in a given time frame was determined by the ice velocity together with ice thickness. 12 m is also where the 1st, 3rd and 5th natural mode frequencies were clearly visible in the response spectral analysis. When moving lower in the vertical direction, first the 5th and then the 3rd mode frequency both disappeared until at water level only the first mode was present in the acceleration response. Based on these results, the horizontal acceleration at the top of the channel marker would be the best for both i) defining the correlation between ice loads and vibration response and ii) capturing the natural mode frequencies present in the channel marker dynamic response.

Because we do not yet have any measurements of the structure, there exist several sources for uncertainties in the structural model. The most important uncertainty factors are related to the seabed properties (soil-structure interaction) and the damping due to water and soil. These have significant influence on the dynamic properties of the structure. The structural model will be updated and simulations reanalyzed after the dynamic system is identified experimentally.

ACKNOWLEDGEMENTS

The authors gratefully acknowledge Terramare-Boskalis, Labkotec Oy, Skarta Energy Oy, Skyborn Renewables AB, OX2 and Metsähallitus for funding the SBP-IceWind project. The authors also gratefully acknowledge the Academy of Finland for funding the WindySea project (Special RRF funding for research on key areas of green and digital transition [grant number 348588]).

Mika Lehtola and Antti Pihlaja from Vayla and Jukka Törmänen from Ponvia are acknowledged for providing information about the channel marker.

REFERENCES

Bjerkås, M., 2006. Ice action on offshore structures. PhD Thesis In: NTNU, ISBN 82-471-7756-0, 173 pp.

Bjerkås, M. & Nord, T.S. 2016. Ice action on Swedish lighthouses revisited. IAHR International symposium on ice.

Brown, T.G. & Määttänen, M. 2009. Comparison of Kemi-I and Confederation Bridge cone ice load measurement results. Cold Regions Science and Technology 55 (2009) 3–13

Li, H., Bjerkås, M., Høyland, K.V., Nord, T.S., 2016. Panel loads and weather conditions at Norströmsgrund lighthouse 2000–2003. In: 23rd IAHR International Symposium on Ice Ann Arbor, Michigan, USA, pp. 10 ISSN: 2414-6331.

Høyland, K.V., Nord, T.S., Hendrikse, H., Tuhkuri, J., Polojärvi, A., von Bock und Polach, F., Heinonen, J., Eik, K., Teigen, S, Serré, N., Schümann, B., von Borstel, T., Reimer, N., Haase, A. and Sjöblom, A. 2023. Challenges with sea ice action on structures for Offshore wind. Proceedings of the 27th International Conference on Port and Ocean Engineering under Arctic Conditions, 12-16 June 2023, Glasgow, United Kingdom

Hoikkanen, J. 1985. Measurements and Analysis of Ice Force against a Conical Offshore Structure. Proceedings of the International Conference on Port and Ocean Engineering under Arctic Conditions, POAC. 1985.

https://www.openstreetmap.org/

Leppäranta, M., & Myrberg, K., 2009. Physical Oceanography of the Baltic Sea. Springer.

Määttänen, M., Mustamäki, E. 1985. Ice forces exerted on a conical structure in the Gulf of Bothnia. Offshore Technology Conference OTC 5054, Houston, USA

Määttänen, M., 1986. Test cone project, Proc. Polartech '86, VTT symposium 71, Espoo pp. 749-761

Nord, T.S., Samardžija, I., Hendrikse, H. Bjerkås, M., Høyland, K.V. Li, H. 2018. Ice-induced vibrations of the Norströmsgrund lighthouse, Cold Regions Science and Technology, Volume 155, 2018, Pages 237-251, ISSN 0165-232X, https://doi.org/10.1016/j.coldregions.2018.08.005.

Nord, T.S., Øiseth, O., Petersen, Ø. and Lourens, E-M. 2015. Sensor network for dynamic ice-force identification: The Hanko-1 channel marker case study. Proceedings of the International Conference on Port and Ocean Engineering under Arctic Conditions, POAC. 2015.

Nordlund, O.P., Kärnä, T., Järvinen, E. 1988. Measurements of Ice-Induced Vibrations of Channel Markers. IAHR Ice Symposium, Sapporo, Japan (1988), pp. 537-548

Tikanmäki, M, Heinonen, J, Montonen, A & Eriksson, PB. 2019. Ice condition parameters of the Gulf of Bothnia with relation to offshore wind turbine design. in Proceedings of the 25th International Conference on Port and Ocean Engineering under Arctic Conditions, POAC 2019, Delft, Netherlands

Turunen, R., Nordlund, O.P. 1988. Full-Scale Measurements of the Dynamic Properties of a Channel Marker. IAHR Ice Symposium, Sapporo, Japan (1988), pp. 549-560